Cooperative Effects Dominating the Thermodynamics and Kinetics of Surfactant Adsorption in Porous Media: From Lateral Interactions to Surface Aggregation

Zaineb Zaafouri, Daniela Bauer, Guillaume Batôt, Carlos Nieto-Draghi, Benoit Coasne

Cooperative Effects Dominating the Thermodynamics and Kinetics of Surfactant Adsorption in Porous Media: From Lateral Interactions to Surface Aggregation

Zaineb Zaafouri, Daniela Bauer,* Guillaume Batôt, Carlos Nieto-Draghi, and Benoit Coasne*

ABSTRACT: Surfactant adsorption in porous media remains poorly understood, as the microscopic collective behavior of these amphiphilic molecules leads to nonconventional phenomena with complex underlying kinetics/structural organization. Here, we develop a simple thermodynamic model, which captures this rich behavior by including cooperative effects to account for lateral interactions between adsorbed molecules and the formation of ordered or disordered self-assemblies. In more detail, this model relies on a kinetic approach, involving adsorption/desorption rates that depend on the surfactant surface concentration to account for facilitated or hindered adsorption at different adsorption stages. Using different surfactants/porous solids, adsorption on both strongly and weakly adsorbing surfaces is found to be accurately described with parameters that are readily estimated from available adsorption experiments. The validity of our physical approach is confirmed by showing that the inferred adsorption/desorption rates obey the quasi-chemical approximation for lateral adsorbate interactions. Such cooperative effects are shown to lead to adsorption kinetics that drastically depart from conventional frameworks (e.g., Henry, Langmuir, and Sips models).

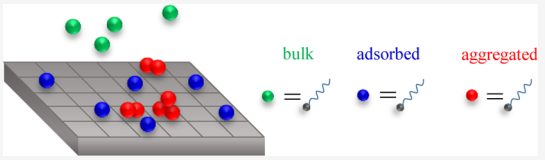

1. INTRODUCTION

Surfactants, which are amphiphilic molecules combining a hydrophilic head with a hydrophobic tail, constitute an important class in Soft Matter. Besides their ability to decrease surface tension by getting adsorbed at interfaces, an important property of surfactants in water is to exhibit a complex phase diagram including a miscibility gap (a temperature/concentration range where demixing occurs from water).[1] Even in the miscibility region, there exists a critical micelle concentration (cmc) above which surfactants form ordered mesoscopic assemblies—typically spherical micelles where the surfactant tails are inside the micelle, while polar or charged heads are at the micelle external surface in contact with water (Figure 1). Owing to their tendency to form micelles and reduce surface tension, surfactants are at the heart of many applications where they are used as detergents, dispersants, emulsifiers, and so forth.[2−4] In particular, in heterogeneous solutions such as oil/water systems, they are used to trap oil droplets inside the core of surfactant micelles. In many situations, such a phase separation occurs in porous media or in the vicinity of solid surfaces, an important example being the use of surfactants to untrap important oil amounts located in oil reservoirs/rocks.[5−7]

The rich thermodynamic behavior of surfactants results from competing molecular interactions between the different—hydrophobic and hydrophilic—groups, which combine with large entropy effects for such molecules.[8] However, despite such an intrinsic complexity, the phase behavior of bulk surfactants is reasonably well understood with available formalisms to describe phenomena such as self-assembly and phase separation/transition and also nonintuitive temperature effects on liquid immiscibility, solubility, and micellization.[9−11] In contrast, the physical behavior of surfactants confined in porous materials or close to solid surfaces still challenges existing frameworks.[12] Adding free energy contributions resulting from the head/surface and tail/surface intermolecular interactions leads to intriguing effects such as inverse temperature adsorption and also surface transitions between disordered and/or ordered mesoscopic assemblies (e.g., bilayers, hemi-micelles, vesicles, and elongated micelles).[9,13−15] The situation is even more puzzling as the observed adsorption type depends specifically on the solid chemistry (e.g., surface affinity/groups with possible amphoteric charges), surfactant molecules (e.g., apolar/polar, cationic/anionic), and thermodynamic/solution conditions (e.g., concentration, temperature, and presence of an electrolyte).[16−19]

As a result of this complexity, most of the experimental literature on surfactant adsorption focuses on a given family of surfaces or surfactants. In particular, significant research effort has been devoted to unraveling the structural mechanisms followed upon adsorption at increasing concentrations.[20−24] By

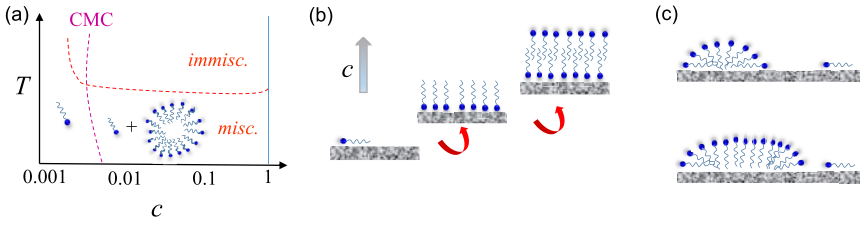

Figure 1. (a) Temperature−concentration (T, c) phase diagram of bulk surfactant solutions. The surfactant monomer is pictured as a hydrophilic head (blue sphere) combined with a hydrophobic chain (grey segment). A miscibility gap separates the high/low T regions with solvent/surfactant miscibility only observed at low T and c. In the miscibility range, for c smaller than the so-called cmc, the monomers are solubilized in the solvent phase. For c > cmc, the monomers coexist with micelles. (b,c) Orientation of surfactant molecules and possible surface aggregates obtained at a solid surface. (b) corresponds to the stepped Langmuir adsorption isotherm with the formation of an adsorbed monomer layer followed by film reorientation and growth. (c) illustrates other ordered or disordered self-assemblies coexisting with isolated adsorbed monomers.

combining thermodynamic measurements with structural analysis, some authors proposed advanced scenarios to rationalize step adsorption and/or S-shaped adsorption isotherms observed experimentally.[25,26] As illustrated in Figure 1b, such mechanisms involve the adsorption of isolated monomers followed by the formation of a monolayer, which eventually transforms into more complex structures (e.g., bilayer, hemimicelle, and vesicle) upon increasing the surfactant concentration.[27] However, although such combined structural/thermodynamical studies provide a robust description for a broad class of solid/surfactant situations, there is a number of systems that lead to more complex data departing from such a generic picture.[28,29] In particular, data for surfactants in various silica-based porous materials display complex adsorption mechanisms and kinetics involving the formation of elongated/distorted micelles or vesicles [as illustrated in Figure 1c] that cannot be captured using currently available models. Such complex effects arise from the heterogeneity in the solid surface chemistry and disordered morphology/topology of the host confining material.

From a theoretical viewpoint, statistical physics is a powerful framework to predict the complex behavior of surfactants in bulk solution (including anomalous temperature effects on self-assembly for instance). In particular, extended lattice gas theory for monomers including a supralattice for the formation of micelles was shown to capture most of the physical phenomena involved in the phase diagram of these complex objects.[30] This method was extended later by Bock and Gubbins[31] to account for surface adsorption through the use of surface interaction terms in the lattice gas Hamiltonian.[30] From a thermodynamic viewpoint, several models such as those described hereafter have been proposed to describe surfactant adsorption on solid surfaces. Empirical models have been proposed to describe in an effective fashion the S-shaped adsorption isotherms. This is the essence of the Sips model,[32] which corresponds to the Langmuir model with the pressure raised to an empirical power α. The Toth model falls in the same category, as it consists of accounting empirically for surface heterogeneity through a stretched Langmuir adsorption isotherm.[33] Other empirical approaches in this field consist of combining different physical models such as Henry, Langmuir, and BET adsorption isotherms to account for nonconventional surfactant adsorption isotherms.[34] More physical pictures have been proposed such as the model by Zhu and Gu, in which adsorption is described as a two-step process with two underlying equilibrium conditions (single-monomer adsorption and monomer recombination to form self-assemblies).[35,36] Other physical models such as those proposed by Temkin[37] and Reed−Ehrlich[38] rely on the quasi-chemical approximation to account for lateral interactions within the adsorbed layer. This approximation is an extension of the Bragg−Williams approximation, in which the Langmuir model is augmented by including a mean-field description of the lateral interactions between adsorbed molecules.[39]

In spite of their physical basis, the models described above do not provide a general formalism for surfactant adsorption, as they address different aspects (lateral interaction or self-assembly). In other words, a reliable thermodynamic description of the behavior of surfactants at surfactant/surface interfaces should include both lateral interactions and transitions from adsorbed monomers to self-assembled objects. This task is complex but also crucially needed, as the specific adsorption type observed experimentally depends on many parameters (surfactant type, surface chemistry, presence of electrolytes/other fluid components, etc.). Here, we intend to fill this gap by providing a generic theoretical picture of surfactant adsorption through a phenomenological model based on simple thermodynamic ingredients. In more detail, this physical model is obtained by including physical cooperative effects that account for both lateral interactions between adsorbed molecules and self-assembly at the solid surface through a site occupancy parameter that can be larger than unity. It is important to recognize here that simply accounting for lateral interactions in adsorption models is not sufficient to describe the adsorption of mesoscopic objects at the solid surface (even if such lateral interactions are physically needed to account for self-assembly, a site occupancy >1 must be considered to describe the adsorption of supramolecular structures).

In practice, this model is derived by writing a constitutive kinetic equation involving adsorption/desorption rates that are dependent on the surfactant surface concentration to account for facilitated or hindered adsorption. Using experimental data for two surfactants on two mineral surfaces, this simple yet realistic model is shown to capture different surfactant adsorption types as observed upon varying the surfactant affinity toward the surface. We note that the present model can be extended to almost any surfactant adsorption/porous surface type, as it has its roots in generic thermodynamic concepts (fluid/surface affinity, occupancy/packing, fluid/fluid interactions, etc.). The cooperative effects invoked in our model to capture the complex adsorption phenomena occurring at the surfactant/surface interface are believed to be physically relevant as they can be rationalized using a simple quasi-chemical adsorption model (which can be seen as a Langmuir model in which interactions between adjacent

adsorbed molecules are treated in a mean-field approximation). It is also shown that the adsorption kinetics is drastically affected by such cooperative effects, therefore offering an additional mean to understand the physics of surfactant adsorption (driving forces corresponding to lateral interactions and surface self-assembly).

2. THERMODYNAMIC MODEL

To derive our model, let us consider the situation depicted in Figure 2 with a solid surface made up of adsorption sites

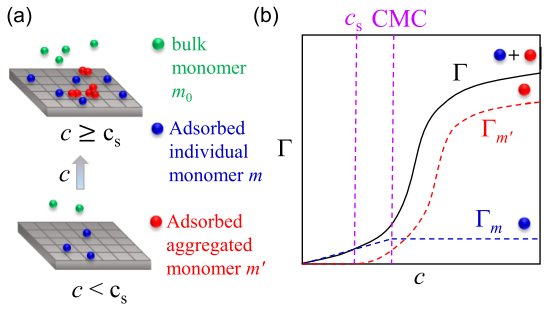

Figure 2. (a) Thermodynamic model of surfactant adsorption onto a solid surface in which the surface concentration Γ as a function of the bulk concentration c is the sum of a contribution Γ_m corresponding to adsorbed individual monomers m and a contribution $\Gamma_{m'}$ corresponding to aggregated monomers m'. (b) Adsorption isotherm corresponding to the model shown in (a). The black line is the total surface concentration Γ, while the blue and red lines correspond to Γ_m and $\Gamma_{m'}$, respectively. For bulk concentration c smaller than the critical surface concentration c_s, only isolated monomers m get adsorbed at the surface—here following a Henry adsorption isotherm $\Gamma_m \sim c$ but any other adsorption regime can be considered. For $c >$ cmc, Γ_m plateaus as the bulk concentration of isolated monomers remains constant. For $c_s < c <$ cmc, both isolated monomers m and monomers in aggregated objects m' adsorb at the surface.

denoted as s. Each site s can adsorb a single monomer m (blue sphere) or $n = 1/\beta$ aggregated monomers m' (red sphere), where n can be seen as the packing efficiency of aggregated monomers. $\beta \in [0, 1]$ is a key ingredient which renders our model versatile, as it allows describing very different physical situations. $\beta = 1/n$ describes the physical situation previously considered by Zhu and Gu,[35] where a single monomer is used to aggregate with $n - 1$ other monomers to form a column on a single solid site s. In contrast, $\beta \to 1$ corresponds to very weakly aggregated object, where each monomer m' lies at a solid site s. Therefore, as will be illustrated in the present paper, defining β as a variable allows reproducing—at least in an effective fashion—almost any aggregation type without having to assume a given shape (micelle, hemi-micelle, vesicle, disordered aggregate, etc.). In particular, the combined use of a packing efficiency and surface concentration adsorption constants allows describing both the adsorption of aggregated monomers forming at the pore surface (below and above cmc) and the direct adsorption of micelles formed in the bulk solution (above cmc).

Having introduced the fundamental ingredients of our model, its constitutive equations for adsorption equilibrium and kinetics can be derived by writing simple mass-balance equations between the free monomers m_0 (green spheres) in solution $c = c[m_0]$, the solid surface sites s, the adsorbed individual monomers m, and the adsorbed aggregated monomers m'. Although such conditions can be written formally, rendering our model tractable requires an additional assumption as follows. We introduce a surface critical concentration c_s below which only individual monomers m adsorb—this critical concentration can be seen as a minimum concentration to observe the formation of aggregated (self-assembled) structures at the solid surface. In this range, $c < c_s$, surface phase equilibrium can be expressed as $s + m_0 \rightleftharpoons m$ with the underlying first-order kinetic equilibrium given by

$$\frac{\partial \Gamma_m(c, t)}{\partial t} = k_A c[\Gamma^\infty - \Gamma_m(c, t)] - k_D \Gamma_m(c, t) \quad (1)$$

where $\Gamma_m(c, t)$ is the surface concentration of individual adsorbed monomers m and Γ^∞ is the surface site concentration in which individual monomers m can adsorb. The first and second terms in the right hand side of eq 1 account for the adsorption/desorption contributions over a time ∂t (k_A and k_D are the adsorption and desorption rates, respectively). The solution to this well-known mass-balance condition corresponds to the Langmuir kinetics (with $k = k_A/k_D$)

$$\Gamma_m(c, t) = \frac{\Gamma^\infty ck}{1 + ck}[1 - e^{-(1+k)k_D t}] \quad (2)$$

which converges in the stationary regime ($t \to \infty$) toward the Langmuir model $\Gamma_m(c, \infty) = \Gamma^\infty ck/(1 + ck)$. In passing, we note that taking the limit $\Gamma^\infty \gg \Gamma_m(c, \infty)$ allows recovering the Henry regime as usually observed at very low concentrations c: $\Gamma_m(c, t) = \Gamma^\infty ck[1 - e^{-k_D t}]$ with the long-time limit $\Gamma_m(c, \infty) = \Gamma^\infty ck$.

For $c \geq c_s$, both the individual monomers m and aggregated monomers m' adsorb in the surface sites s. As already mentioned, using the concept of aggregated monomers, we encompass into the same contribution, both the adsorption and recombination of adsorbed surfactants into mesoscopic assemblies (for $c > c_s$) and the direct adsorption of micelles formed in the bulk onto the solid surface (for $c >$ cmc $> c_s$). This is a specificity of our model in which the use of surface concentration-dependent adsorption/desorption rates allows treating in an effective yet physical fashion these complex adsorption phenomena. Here, as a simplification that allows straightforward comparison with experimental data without changing fundamentally the physical basis of our model, we assume that the adsorption of individual monomers m occurs on a much shorter timescale than the adsorption of aggregated monomers m'. This implies that in the following kinetic equation, $\Gamma_m(c, t) \sim \Gamma_m(c, \infty)$ $\forall t$. Moreover, each surface site is assumed to adsorb $n = 1/\beta$ aggregated monomers where the packing efficiency n allows accounting for nearly any self-assembled object. With these approximations, surface phase equilibrium for $c \geq c_s$ can be expressed as $s^* + m_0 \rightleftharpoons m'$ where * in s^* indicates that only the surface sites that remain available for aggregated monomers m' are considered. The corresponding first-order kinetic equation for the adsorption/desorption of the aggregated monomers m' in such a process can be expressed as

$$\frac{\partial \Gamma_{m'}(c, t)}{\partial t} = k'_A(\Gamma_{m'})c \times [\Gamma^\infty - \Gamma_m(c, \infty) - \beta\Gamma_{m'}(c, t)] - k'_D(\Gamma_{m'})\Gamma_{m'}(c, t) \quad (3)$$

where $\Gamma_{m'}(c, t)$ is the surface concentration in aggregated monomers m', while β accounts for the fact that the adsorption of a single monomer in aggregated objects only occupies a fraction β of the surface site (therefore, with these definitions,

$\beta\Gamma_{m'}(c, t)$ is the number of such mesoscopic, i.e., aggregated, objects). Moreover, to account for lateral interactions between monomers in aggregated objects, we make the adsorption and desorption rates k'_A and k'_D in the abovementioned equation explicitly dependent on the surface concentration $\Gamma_{m'}$. At equilibrium (i.e., in the stationary regime $\partial\Gamma_{m'}/\partial t = 0$), for a bulk concentration c, this kinetic equation leads to the following solution

$$\Gamma_{m'}(c, \infty) = [\Gamma^{\infty} - \Gamma_m(c, \infty)] \times k'(\Gamma_{m'})c/[1 + \beta ck'(\Gamma_{m'})] \quad (4)$$

where $k'(\Gamma_{m'}) = k_{A'}(\Gamma_{m'})/k'_D(\Gamma_{m'})$.

In summary, this model allows introducing a required degree of complexity through collective effects in surfactant adsorption that manifest themselves into two factors. First, although isolated monomers are assumed to adsorb independently of each other, lateral interactions between monomers adsorbing into self-assemblies must be included. Second, the formation of either ordered (e.g., hemimicelle and vesicle) or distorted (e.g., elongated micelle) mesoscopic assemblies is included in an effective fashion through the use of a packing efficiency n. This generic model relies on a limited yet important set of assumptions, namely, superimposition of isolated and aggregated monomer adsorption, fast-isolated monomer adsorption, and description of self-assemblies through an effective parameter n. However, despite these assumptions, as illustrated in the remaining of this paper, this model allows deriving fundamental insights into the thermodynamics and kinetics of surfactant adsorption from simple experimental data. In particular, as shown below, a merit of this model is that the adsorption-dependent dynamical coefficients governing the adsorption kinetics of isolated and aggregated monomers can be estimated from static adsorption data (because the adsorption/desorption rates k'_A and k'_D depend explicitly only on $\Gamma_{m'}$). Moreover, this versatile model can be applied with almost no restriction regarding the type of surfactants, surfaces, self-assemblies, thermodynamic conditions, and so forth.

3. RESULTS AND DISCUSSION

To test our model, we consider two sets of experimental data, which are representatives of different surfactant adsorption behaviors. In more detail, we use the data by Denoyel and Rouquerol who considered the adsorption at room temperature of two polar (nonionic) surfactants onto silica-based surfaces (TX100 onto silica and TX165 onto kaolinite clay).[21] As shown in Figure 3, for both systems, the adsorption isotherms exhibit two regimes, which correspond to monomer adsorption at low concentrations c followed by a rapid increase in the surface concentration, corresponding to surface self-assembly at concentrations around the cmc. However, a major difference between the two datasets lies in the monomer adsorption regime in the low concentration range with a slow—Henry-like—regime for Figure 3a and a rapid—Langmuir-like—regime for Figure 3b (we note that in general, a Langmuir model can be assumed by default, as the Henry law is simply its asymptotic limit). Because the two surfactants considered here are similar nonpolar molecules with an OH group at their end, the origin of this difference has to be found in the surface chemistry of the different surfaces. Typically, for the kaolin sample, as discussed by Denoyel and Rouquerol,[21] the observed strong adsorption phenomenon is thought to occur on a basal plane—more exactly, the basal plane made up

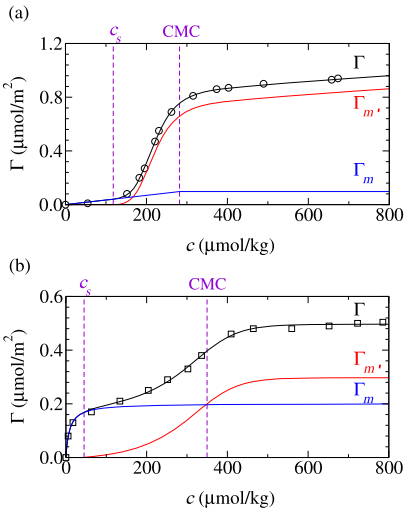

Figure 3. Surfactant adsorption isotherms at T = 298 K showing the surface concentration of surfactants Γ onto a silica-based surface as a function of the bulk concentration c: (a) TX100 surfactant on quartz silica and (b) TX165 surfactant on kaolin. The black symbols are the experimental data taken from Denoyel and Rouquerol[21] with the black line corresponding to smoothed interpolation data. For both systems, the blue and red lines show the predictions of our model for the adsorption of isolated and aggregated monomers, respectively (by construction, the sum of these two contributions is equal to the experimental data). A Henry law and a Langmuir law were used to describe the isolated monomer adsorption in (a,b), respectively. The vertical dashed lines indicate the critical surface concentration c_s and cmc.

of aluminol sites, as the surface concentrations were found to be pH-independent (adsorption sites on this basal plane do not form amphoteric charges with pH).[21] In contrast, because the weak adsorption phenomenon displayed in Figure 3 for silica is found to be pH-sensitive, it is assumed to occur on neutral adsorption sites that become charged upon increasing the pH.

We use the following procedure to apply our model to the experimental data $\Gamma^{exp}(c)$ shown in Figure 3. First, to define the surface critical concentration c_s, the interpolated experimental data are fitted against a Langmuir adsorption isotherm over a concentration range $[0, c_{max}]$. Although the fit is accurate for small c_{max}, the fit does not provide satisfactory results for large c_{max} (because a simple Langmuir or Henry adsorption isotherm cannot describe the raw experimental adsorption data over a large-concentration range). At this stage, it is decided to define c_s as the maximum value c_{max}, for which a correlation coefficient of R^2 = 0.99 is obtained. Although the specific cutoff value used is arbitrary, it should be emphasized here that slightly different values would lead to very similar predictions (in practice, with variations in the degree of agreement with experimental data that falls within the experimental error bar). This allows us to have a good approximation to describe the monomer surface concentration $\Gamma_m(c, \infty)$ for $c < c_s$. Here, it is worth mentioning that fitting the Henry or Langmuir model to low-concentration data requires that enough experimental data points are available to ensure rigorous fitting and, hence, robust physical parameterization. As an illustration, Figure S2 shows the different adsorption isotherms obtained as c_s is varied from $c_s \sim 0$ to $c_s >$ cmc. Second, having a fitted model for $\Gamma_m(c, \infty)$, one can estimate the contribution corresponding to the adsorbed aggregated monomers $\Gamma_{m'}(c, \infty)$ by subtracting $\Gamma_m(c, \infty)$ from $\Gamma^{exp}(c)$,

that is, $\Gamma_{m'}(c, \infty) = \Gamma^{exp}(c) - \Gamma_m(c, \infty)$. Third, $k'(\Gamma_{m'})$ can be readily estimated from $\Gamma_{m'}(c, \infty)$ by inverting eq 4

$$k'(\Gamma_{m'}) = \frac{\Gamma_{m'}(c, \infty)}{c[c - \Gamma_m(c, \infty) - \beta\Gamma_{m'}(c, \infty)]} \quad (5)$$

As shown in Figure 3, for both systems, the model including cooperative effects applies accurately to the experimental data. From a practical viewpoint, as described above, applying our model to available experiments requires to determine the following parameters. Although the Langmuir (Henry) constant k_H (k_L) must be fitted together with c_s from the low-concentration range, the maximum adsorbed amount Γ^∞ is determined from the high-concentration range.

Figure 4 shows $k'(\Gamma_{m'})$ as a function of $\Gamma_{m'}$ for the two systems considered here (TX100 on quartz silica and TX165

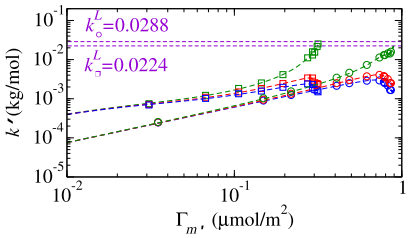

Figure 4. Adsorption constant $k'(\Gamma_{m'})$ for the aggregated monomers m' as a function of their surface concentration $\Gamma_{m'}$, as extracted from the experimental adsorption data shown in Figure 3. The circles are for TX100 adsorption on quartz silica, while the squares are for TX165 on kaolin (experimental data taken from ref 21). For each system, the blue, red, and green data denote data obtained for $\beta = 0.2$, $\beta = 0.5$, and $\beta = 1.0$, respectively. The two horizontal dashed lines in purple indicate the Langmuir adsorption constants that best match the experimental adsorption isotherms in the high-concentration range $c > c_s$.

on kaolin). It should be noted that the model applied to the isothermal adsorption data does not allow estimating β. This is a drawback of our model, but β can be estimated independently of $k'(\Gamma_{m'})$ from adsorption kinetic data, as shown in the last part of this paper. Figure 4 shows that $k'(\Gamma_{m'})$ increases with increasing $\Gamma_{m'}$ for a given β, therefore pointing to the existence of collective, that is, cooperative, effects in surfactant adsorption (otherwise $k'(\Gamma_{m'})$ would remain constant). Physically, this behavior indicates that cooperative effects lead to enhanced adsorption with already-adsorbed molecules, facilitating adsorption of additional monomers either in the same adsorption sites (when $\beta \neq 1$) and/or in neighboring adsorption sites ($\beta = 1$). As expected from eq 5, upon decreasing β, the fraction of available sites to adsorb aggregated monomers increases, so that $k'(\Gamma_{m'})$ decreases. This is due to the fact that $k'(\Gamma_{m'})$ is an effective adsorption constant, so that low β corresponds to systems that tend to self-assemble easily (therefore not requiring large adsorption constants to pack efficiently at the solid surface). Figure 4 also shows for the two systems considered here the Langmuir adsorption constant $k^L = k_A/k_D$, which was estimated by fitting the concentration range beyond the critical surface concentration $c > c_s$. In more detail, by restricting the fitting procedure to the region where the surface concentration increases rapidly with concentration, it is possible to describe semiquantitatively the data using a simple Langmuir model with shifted concentrations $\tilde{c} \sim c - c_s$. As shown in Figure 4, except for large surface concentrations $\Gamma_{m'}$, regardless of the system considered, the Langmuir constant k^L overestimates the adsorption constant $k'(\Gamma_{m'})$ predicted using our model (Figure S3 in the Supporting Information shows the fits of the high-concentration experimental data to the Langmuir model). This result is due to the fact that the Langmuir model does not describe cooperative adsorption, so a larger effective constant is needed to capture the increasing adsorption rate upon increasing the surface concentration.

For a given surfactant/surface couple, the parameters involved in the present model are derived from available experimental data. To assess the physical validity and robustness of our model, it is important to connect its underlying parameters to existing theoretical frameworks. In this context, as stated in the Introduction, statistical physics offers an efficient and accurate formalism to describe cooperative adsorption effects. In particular, the quasi-chemical approximation[39] allows deriving a simple expression for the surface concentration that accounts for lateral interactions between adsorbed monomers. Here, for the sake of brevity, we provide the main thermodynamic ingredients of this important model, which goes well beyond the Langmuir model (an exact derivation can be found in the Supporting Information). Let us consider free monomers in a bulk solution that can adsorb onto surface sites. Assuming additive lateral interactions between an adsorbed molecule and its neighbors, the adsorption energy E of a monomer cluster made of x monomers is $E \sim xw$, where w is the interaction with a single neighbor. Phase equilibrium between the adsorbed monomers and the free monomers in solution at a temperature T implies that the chemical potential is equal in the two phases, that is, $\mu = \mu_b$ (the subscript b refers to the bulk solution). In the quasi-chemical approximation, as shown in the Supporting Information, the chemical potential of the adsorbed phase writes $\mu = \mu_0 + k_BT \ln[\theta/(1 - \theta)] + z_0k_BT/2 \ln[(\gamma - 1 + 2\theta)(1 - \theta)/\theta(\gamma + 1 - 2\theta)]$, where $\theta \in [0, 1]$ is the site average occupancy, z_0 is the number of neighboring sites ($z_0 = 4$ for a surface), and $\gamma = [1 - 4\theta(1 - \theta)(1 - \eta)]^{1/2}$ (with $\eta = \exp[-w/k_BT]$). In this expression, the reference chemical potential $\mu_0 = [z_0w/2 + \epsilon_0]/k_BT$ corresponds to the energy of an adsorbed monomer at full saturation (which includes an energy contribution with the surface $\sim\epsilon_0$ and an energy contribution with all neighboring adsorbed monomers $\sim z_0w/2$). By noting that $\theta = \beta\Gamma_{m'}/(\Gamma^\infty - \Gamma_m)$ and $1 - \theta = (\Gamma^\infty - \Gamma_m - \beta\Gamma_{m'})/(\Gamma^\infty - \Gamma_m)$, the previous expression leads to the following expression for $\Delta\mu = \mu - \mu_0$

$$\frac{\Delta\mu}{k_BT} = \ln\left[\frac{\beta\Gamma_{m'}}{\Gamma^\infty - \Gamma_m - \beta\Gamma_{m'}}\right] + \frac{z_0}{2}\ln\left[\frac{\Gamma^\infty - \Gamma_m - \beta\Gamma_{m'}}{\beta\Gamma_{m'}}\right] + \frac{z_0}{2}\ln\left[\frac{(\gamma - 1)(\Gamma^\infty - \Gamma_m) + 2\beta\Gamma_{m'}}{(\gamma + 1)(\Gamma^\infty - \Gamma_m) - 2\beta\Gamma_{m'}}\right] \quad (6)$$

Taking the bulk concentration $c = c_0$ as the concentration at the reference point μ_0 and assuming that the concentration remains low enough, we can write $\Delta\mu$ for the bulk phase as $\Delta\mu_b = k_BT \ln c/c_0$. By inverting eq 5, we obtain $c = 1/k'(\Gamma_{m'}) \times \Gamma_{m'}/[\Gamma^\infty - \Gamma_m - \beta\Gamma_{m'}]$, which leads to the following expression upon insertion in $\Delta\mu_b$

$$\frac{\Delta\mu_b}{k_BT} = \ln\left[\frac{\beta\Gamma_{m'}}{\Gamma^\infty - \Gamma_m - \beta\Gamma_{m'}}\right] - \ln\left[\frac{c_0 \times k'(\Gamma_{m'})}{\beta}\right] \quad (7)$$

To verify that our model of cooperative adsorption is consistent with a description of interacting adsorbed species,

we can check that the chemical potential equality as defined in the quasi-chemical approximation is obeyed. To do so, by noting that the first term on the right-hand side, that is, $\mu^* = k_BT \ln[\beta\Gamma_{m'}/(\Gamma^\infty - \Gamma_m - \beta\Gamma_{m'})]$, is identical in eqs 6 and 7, we can compare $\Delta\mu - \mu^*$ and $\Delta\mu_b - \mu^*$. As shown in Figure 5, when using the values for k' in Figure 4, a good agreement is

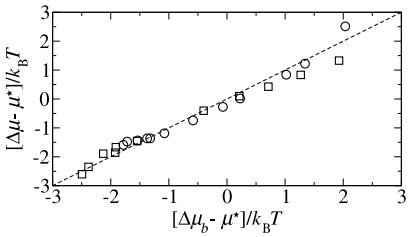

Figure 5. Comparison between the chemical potential shift for bulk and adsorbed surfactants, as predicted within the quasi-chemical approximation using the data derived from our model. The circles and squares refer to the data for TX100 on quartz silica and TX165 on kaolin, respectively (experimental data taken from ref 21). The dashed line is a guide to the eye, which indicates chemical potential equality between the bulk and adsorbed phases.

obtained between the two chemical potentials for both TX100 on quartz silica and TX165 on kaolin. When establishing such a comparison, $\eta = \exp[-w/k_BT]$ and c_0 were used as adjustable parameters, but we note that they are the only fitting variables—we found that $\eta \sim 3.3$ for TX100 on silica and $\eta \sim 4.0$ for TX165 on kaolinite. More importantly, it was verified a posteriori that these values for η, which lead to $w \sim -1.2k_BT$ for TX100 on silica and $w \sim -1.4k_BT$ for TX165 on kaolinite, are physically relevant, as discussed in what follows. First, as expected for cooperative effects leading to facilitated adsorption, w is negative, so that it corresponds to attractive lateral interactions between adsorbed neighbors. Second, w is of the order of k_BT, as required to observe cooperative adsorption (indeed, for lower, i.e., less, negative lateral interactions, thermal motion and therefore desorption would prevail). Third, the stronger attractive interaction w for TX165 is consistent with the fact that this molecule is similar to TX100 but with a longer alkyl chain—16 versus 9−10 carbon groups. In practice, the two datasets used are for different surfaces—which could affect the comparison made here—but we recall that η is related to the interaction between two adsorbed molecules and can, therefore, be considered to be mostly dependent on their molecular nature/chemistry. A few remarks are in order here. First, although our thermodynamic model is found to be consistent with the quasi-chemical approximation, the latter is insufficient to fully describe surfactant adsorption over the whole concentration range. Indeed, the quasi-chemical approximation is only relevant in the concentration range $c > c_s$, where the surfactant aggregates at the solid surface to form mesoscopic structures (which stem from lateral interactions/collective effects). In contrast, in the low-concentration range, such collective effects are assumed to be absent, so the quasi-chemical approximation is not relevant. Second, even if w should formally depend on the surfactant type only, it is expected to be a function of the solid surface nature in practice. Indeed, considering that the quasi-chemical approximation is a mean-field treatment, effective parameters such as w are expected to depend—even if weakly—on the strength/nature of the surfactant/solid interactions (in other words, the lateral interactions in adsorbed surfactants are necessarily mediated to some extent by the solid/surfactant interactions).

As will be shown here, the present model has strong implications in terms of surfactant adsorption/desorption kinetics on surfaces. In particular, changes in the adsorption/desorption rates induce drastic variations in the characteristic time corresponding to the transient regime leading to thermodynamic equilibrium. Although this feature is not specific to our model (because underlying kinetics in the Langmuir and Henry models also depend on the adsorption/desorption constant rates), the introduced concept of $\Gamma_{m'}$ dependence of k_A and k_D leads to rich and complex kinetics. In this respect, it should be emphasized that only such a level of complexity allows capturing the intriguing adsorption kinetics observed experimentally for surfactant adsorption. In particular, all typical non-Langmuirian adsorption dynamics observed in transient adsorption experiments but also in breakthrough curves, which resist available modeling frameworks, point to the existence of cooperative adsorption effects and, more generally, complex collective phenomena.[16] To illustrate the influence of cooperative effects on adsorption kinetics, the dynamical equation given in eq 3 was solved numerically for different bulk concentrations c. For TX100 adsorption on silica, this leads to the time evolution shown in Figure 6 (the same data for TX165 on kaolin are not shown here for the sake of clarity but can be found in Figure S1 in the Supporting Information). Many choices can be made for $k'_A(\Gamma_{m'})$ and $k'_D(\Gamma_{m'})$ because static adsorption data only provide information on $k'(\Gamma_{m'}) = k'_A(\Gamma_{m'})/k'_D(\Gamma_{m'})$. Two

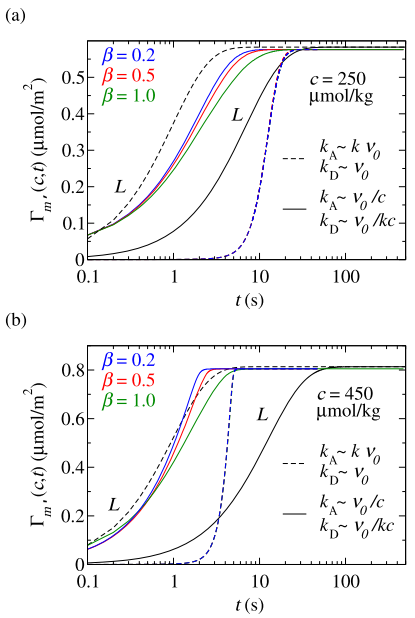

Figure 6. Adsorption kinetics as determined by solving numerically eq 3, showing $\Gamma_{m'}$ as a function of time t for TX100 on silica for two bulk concentrations: (a) $c = 250$ μmol/kg and (b) $c = 450$ μmol/kg. The color lines denote the data obtained using the cooperative model with $\beta = 0.2$ (blue), $\beta = 0.5$ (red), and $\beta = 1.0$ (green), while the black lines correspond to kinetics predicted using the Langmuir kinetic model with an adsorption/desorption constant k^L that best matches the experimental adsorption isotherm (see text). In each case, the dashed lines correspond to the case $k_A \sim \nu_0 k$ and $k_D \sim \nu_0$, while the solid lines correspond to $k_A \sim \nu_0/c$ and $k_D \sim \nu_0/kc$. Note that our model predicts that the color dashed lines (i.e., $k_A \sim k$ and $k_D \sim$ constant) are superimposed.

illustrative situations were considered as shown in Figure 6: (1) $k'_A \sim \nu_0 k'(\Gamma_{m'})$ and $k'_D \sim \nu_0$ and (2) $k'_A \sim \nu_0/c$ and $k'_D \sim \nu_0/k'(\Gamma_{m'})c$, where ν_0 is a characteristic constant in s^{-1} that sets the typical timescale (because it is used as a constant throughout this study, it does not affect the discussion provided below). We emphasize that the two cases considered here are asymptotic limits as both k'_A and k'_D should depend on k' and hence $\Gamma_{m'}$ in general. For each situation, we also consider the effect of the aggregation parameter β, which is varied between $\beta = 0.2$ and 1 ($n = 1/\beta$ is the number of aggregated monomers that can be packed into a single adsorption site). Figure 6 also shows for each situation the kinetics obtained using the Langmuir kinetic model with (1) $k_A^L \sim \nu_0 k^L$ and $k_D^L \sim \nu_0$ and (2) $k_A^L \sim \nu_0/c$ and $k_D^L \sim \nu_0/k^L c$, where k^L is the Langmuir adsorption constant that best matches the experimental adsorption isotherm in the high-concentration range $c > c_s$ (see Figure 4 and its caption).

Examining in detail the two situations considered here allows gaining insights into the role of cooperative effects on surfactant adsorption/desorption kinetics in porous media. In particular, this illustrates how application of the present model to experimental adsorption kinetic data could be used to probe adsorption and desorption properties including the aggregation constant β.

- Case [$k'_A \sim k'$, while $k'_D \sim$ constant]. With these assumptions, inserting the expression for k' given in eq 5 into the kinetics described by eq 3 shows that the adsorption rate k'_A is constant (i.e., independent of β). Therefore, in this case, both k'_A and k'_D are constant, so that the adsorption kinetics is independent of the aggregation parameter β for all concentrations c (see color dashed lines in Figure 6). Moreover, comparison with the ideal Langmuir model for this case indicates that our cooperative model predicts a much slower kinetics as $k' \lesssim k^L$ for all c (as shown in Figure 4). Indeed, at a constant desorption rate, the kinetics becomes faster with increasing adsorption rate.
- Case [$k'_A \sim$ constant, while $k'_D \sim 1/k'$]. With these assumptions, β significantly affects the observed adsorption kinetics. As can be inferred from eq 5, k' increases with β, so that $k'_D \sim 1/k'$ decreases. As can be directly illustrated using a simple Langmuir kinetic equation, the adsorption kinetics becomes slower with decreasing desorption constant k_D while maintaining k_A constant. This interpretation is consistent with the data shown in Figure 6 for $k'_D \sim 1/k'$ and k_A constant, where it is observed that the adsorption kinetics becomes slower with increasing β. Finally, for a given concentration with $k_D \sim 1/k'$ and k_A constant, we observe that the simple Langmuir kinetics is significantly slower than that observed with cooperative effects. This result is consistent with our previous explanation on the role of the desorption rate at constant k_A because $k^L > k'$ for all c leads to $k_D^L < k'_D$ and therefore a slower kinetics for the Langmuir model. Further study is in progress to fully explore the impact of such cooperative effects on adsorption kinetics using available experimental kinetic data.

4. CONCLUSIONS

In conclusion, we developed a simple physical model of the thermodynamics and kinetics of surfactant adsorption onto surfaces that accounts for cooperative effects inherent to such complex objects. By cooperative effects, we refer here to strong lateral interactions between adsorbed surfactants but also intramolecular and intermolecular interactions responsible for their propensity to form mesoscopic (supramolecular) structures. With this model, important collective driving forces that cannot be ignored for such self-assembling molecules are taken into account to describe the nonconventional static and dynamic adsorption behavior observed experimentally when surfactant solutions are set in contact with solid surfaces. Such collective effects are also at the root of surface aggregation at solution/air interfaces, which stems from mutual interactions between adsorbed molecules.[40] This cooperative behavior was also recently discussed in the context of surfactant adsorption at the water/oil interface, where adsorbed oil molecules were found to enhance surfactant adsorption.[41] In practice, the simple thermodynamic model derived in this paper involves a simple kinetic formalism involving adsorption/desorption rates that vary with the surfactant surface concentration. Such a formalism can be extended to any class of objects that is expected to involve adsorption cooperative effects such as ionic liquids,[42] long-chain molecules (e.g., normal alkanes),[43] and so forth. Moreover, although all cases treated here involved a surface concentration c_s lower than the cmc, our model also deals without any further development to nonwetting situations where surface aggregation occurs beyond its bulk counterpart. The fact that, in all cases, the adsorption isotherm reaches a plateau at a concentration close to the cmc can be rationalized as follows. The cmc corresponds to the chemical potential at which the surfactants in bulk solution condense to form dense surfactant objects (micelles). Within perturbation theory, near a solid surface, the chemical potential where such condensation occurs can be written as the bulk value shifted by a surface interaction contribution.

Once applied to available experimental data, this framework provides a valuable tool to infer key quantities that govern the microscopic behavior of any adsorbed surfactant onto various solid surfaces including surface self-assembly into ordered or disordered structures. More generally, this robust and versatile model, which is found to be consistent with rigorous microscopic treatments such as the quasi-chemical approximation in statistical physics of surface adsorption, can be extended in principle to surfactant adsorption but also transport in porous materials. Beyond immediate practical implications, the results reported here about the nonstandard surfactant adsorption thermodynamics and kinetics in porous materials also raise new challenging questions. In particular, owing to cooperative effects in surfactant adsorption, strong departure from the adsorption/dynamics interplay observed for more classical fluids is to be expected in agreement with experimental observations in breakthrough or injection experiments. This issue is particularly important, as diffusion is usually considered as the main transport mechanism leading to adsorption on surfaces. The present work offers a well-grounded thermodynamic basis to address such questions.

■ ASSOCIATED CONTENT

Supporting Information

The Supporting Information is available free of charge at https://pubs.acs.org/doi/10.1021/acs.jpcb.0c08226.

Description of the quasi-chemical approximation and additional data on the influence of cooperative effects on adsorption kinetics for TX165 on kaolinite (PDF)

AUTHOR INFORMATION

Corresponding Authors

Daniela Bauer − *IFP Energies Nouvelles, 92852 Rueil Malmaison, France*; Email: daniela.bauer@ifpen.fr

Benoit Coasne − *Université Grenoble Alpes, CNRS, LIPhy, 38000 Grenoble, France*; orcid.org/0000-0002-3933-9744; Email: benoit.coasne@univ-grenoble-alpes.fr

Authors

Zaineb Zaafouri − *IFP Energies Nouvelles, 92852 Rueil Malmaison, France; Université Grenoble Alpes, CNRS, LIPhy, 38000 Grenoble, France*

Guillaume Batôt − *IFP Energies Nouvelles, 92852 Rueil Malmaison, France*

Carlos Nieto-Draghi − *IFP Energies Nouvelles, 92852 Rueil Malmaison, France*; orcid.org/0000-0001-5956-9259

Complete contact information is available at: https://pubs.acs.org/10.1021/acs.jpcb.0c08226

Notes

The authors declare no competing financial interest.

ACKNOWLEDGMENTS

The authors are grateful to Elise Lorenceau and Julie Wolanin from Laboratoire Interdisciplinaire de Physique for helpful comments. Z.Z. acknowledges Ph.D. funding at Univ. Grenoble Alpes from IFP Energies Nouvelles.

REFERENCES

(1) Rosen, M. J.; Kunjappu, J. T. *Surfactants and Interfacial Phenomena*; John Wiley & Sons Inc.: Hoboken, New Jersey, 2012.

(2) Raffa, P.; Wever, D. A. Z.; Picchioni, F.; Broekhuis, A. A. Polymeric Surfactants: Synthesis, Properties, and Links to Applications. *Chem. Rev.* **2015**, *115*, 8504−8563.

(3) Ruiz-Ángel, M. J.; Carda-Broch, S.; Torres-Lapasió, J. R.; García-Álvarez-Coque, M. C. Retention Mechanisms in Micellar Liquid Chromatography. *J. Chromatogr. A* **2009**, *1216*, 1798−1814.

(4) Olkowska, E.; Polkowska, Z.; Namieśnik, J. Analytics of Surfactants in the Environment: Problems and Challenges. *Chem. Rev.* **2011**, *111*, 5667−5700.

(5) Bera, A.; Kumar, T.; Ojha, K.; Mandal, A. Adsorption of Surfactants on Sand Surface in Enhanced Oil Recovery: Isotherms, Kinetics and Thermodynamic Studies. *Appl. Surf. Sci.* **2013**, *284*, 87−99.

(6) Kathel, P.; Mohanty, K. K. Wettability Alteration in a Tight Oil Reservoir. *Energy Fuels* **2013**, *27*, 6460−6468.

(7) Zhou, Y.; Wu, X.; Zhong, X.; Sun, W.; Pu, H.; Zhao, J. X. Surfactant-Augmented Functional Silica Nanoparticle Based Nanofluid for Enhanced Oil Recovery at High Temperature and Salinity. *ACS Appl. Mater. Interfaces* **2019**, *11*, 45763−45775.

(8) Israelachvili, J. N. *Intermolecular and Surface Forces*; Academic Press: London, San Diego, 1991.

(9) Soni, S. S.; Sastry, N. V.; Joshi, J. V.; Seth, E.; Goyal, P. S. Study on the Effects of Nonelectrolyte Additives on the Phase, Thermodynamics, and Structural Changes in Micelles of Silicone Surfactants in Aqueous Solutions From Surface Activity, Small Angle Neutron Scattering, and Viscosity Measurements. *Langmuir* **2003**, *19*, 6668−6677.

(10) Strey, R. I. Experimental Facts: Water-Nonionic Surfactant Systems, and the Effect of Additives. *Ber. Bunsen Ges. Phys. Chem.* **1996**, *100*, 182−189.

(11) Corti, M.; Degiorgio, V.; Zulauf, M. Nonuniversal Critical Behavior of Micellar Solutions. *Phys. Rev. Lett.* **1982**, *48*, 1617.

(12) Wilcoxon, J. P.; Martin, J. E.; Odinek, J. Anomalous Phase Separation Kinetics Observed in a Micelle Solution. *Phys. Rev. Lett.* **1995**, *75*, 1558.

(13) Atkin, R.; Craig, V. S. J.; Biggs, S. Adsorption Kinetics and Structural Arrangements of Cationic Surfactants on Silica Surfaces. *Langmuir* **2000**, *16*, 9374−9380.

(14) Király, Z.; Findenegg, G. H. Calorimetric Study of the Adsorption of Short-Chain Nonionic Surfactants on Silica Glass and Graphite: Dimethyldecylamine Oxide and Octyl Monoglucoside. *Langmuir* **2000**, *16*, 8842−8849.

(15) Lugo, D.; Oberdisse, J.; Karg, M.; Schweins, R.; Findenegg, G. H. Surface Aggregate Structure of Nonionic Surfactants on Silica Nanoparticles. *Soft Matter* **2009**, *5*, 2928−2936.

(16) Kwok, W.; Nasr-El-Din, H. A.; Hayes, R. E.; Sethi, D. Static and Dynamic Adsorption of a Non-Ionic Surfactant on Berea Sandstone. *Colloids Surf., A* **1993**, *78*, 193−209.

(17) Denoyel, R.; Giordano, F.; Rouquerol, J. Thermodynamic Study of Non-Ionic—Anionic Surfactant Mixtures: Micellization and Adsorption on Silica. *Colloids Surf., A* **1993**, *76*, 141−148.

(18) Zhang, R.; Somasundaran, P. Advances in Adsorption of Surfactants and their Mixtures at Solid/Solution Interfaces. *Adv. Colloid Interface Sci.* **2006**, *123−126*, 213−229. , Special Issue in Honor of Dr. K. L. Mittal

(19) Penfold, J.; Thomas, R. K. Probing Surfactant Adsorption at the Solid−Solution Interface by Neutron Reflectometry. *Interface Sci. Technol.* **2007**, *14*, 87−115.

(20) Levitz, P.; Van Damme, H. Fluorescence Decay Study of the Adsorption of Nonionic Surfactants at the Solid-Liquid Interface. 2. Influence of Polar Chain Length. *J. Phys. Chem.* **1986**, *90*, 1302−1310.

(21) Denoyel, R.; Rouquerol, J. Thermodynamic (Including Microcalorimetry) Study of the Adsorption of Nonionic and Anionic Surfactants onto Silica, Kaolin, and Alumina. *J. Colloid Interface Sci.* **1991**, *143*, 555−572.

(22) Penfold, J.; Staples, E.; Tucker, I.; Cummins, P. Adsorption of Nonionic Surfactants on Silica Sol Particles: The Effects of Sol Type and Concentration, Surfactant Type, Concentration, and Temperature. *J. Phys. Chem.* **1996**, *100*, 18133−18137.

(23) Qiao, Y.; Schönhoff, M.; Findenegg, G. H. 2H NMR Investigation of the Structure and Dynamics of the Nonionic Surfactant C12E5 Confined in Controlled Pore Glass. *Langmuir* **2003**, *19*, 6160−6167.

(24) Shin, T. G.; Müter, D.; Meissner, J.; Paris, O.; Findenegg, G. H. Structural Characterization of Surfactant Aggregates Adsorbed in Cylindrical Silica Nanopores. *Langmuir* **2011**, *27*, 5252−5263.

(25) Levitz, P. E. Adsorption of Non Ionic Surfactants at the Solid/Water Interface. *Colloids Surf., A* **2002**, *205*, 31−38.

(26) Findenegg, G. H.; Eltekov, A. Y. Adsorption Isotherms of Nonionic Surfactants in SBA-15 Measured by Micro-Column Chromatography. *J. Chromatogr. A* **2007**, *1150*, 236−240.

(27) Esumi, K.; Ueno, M. *Structure-Performance Relationships in Surfactants*; Taylor & Francis Inc.: Bosa Roca, United States, 2003; Vol. *112*.

(28) Oberdisse, J. Small Angle Neutron Scattering and Model Predictions for Micelle-Decorated Colloidal Silica Beads. *Phys. Chem. Chem. Phys.* **2004**, *6*, 1557−1561.

(29) Lugo, D. M.; Oberdisse, J.; Lapp, A.; Findenegg, G. H. Effect of Nanoparticle Size on the Morphology of Adsorbed Surfactant Layers. *J. Phys. Chem. B* **2010**, *114*, 4183−4191.

(30) Vause, C. A.; Walker, J. S. Effects of Orientational Degrees of Freedom in Closed-Loop Solubility Phase Diagrams. *Phys. Lett. A* **1982**, *90*, 419−424.

(31) Bock, H.; Gubbins, K. Anomalous Temperature Dependence of Surfactant Self-Assembly From Aqueous Solution. *Phys. Rev. Lett.* **2004**, *92*, 135701.

(32) Sips, R. On the Structure of a Catalyst Surface. II. *J. Chem. Phys.* **1950**, *18*, 1024−1026.

(33) Toth, J. State Equation of the Solid-Gas Interface Layers. *Acta Chim. Hung.* **1971**, *69*, 311−328.
(34) Redlich, O.; Peterson, D. L. A Useful Adsorption Isotherm. *J. Phys. Chem.* **1959**, *63*, 1024.
(35) Zhu, B.-Y.; Gu, T. General Isotherm Equation for Adsorption of Surfactants at Solid/Liquid Interfaces. Part 1. Theoretical. *J. Chem. Soc., Faraday Trans. 1* **1989**, *85*, 3813−3817.
(36) Zhu, B.-Y.; Gu, T. Surfactant Adsorption at Solid-Liquid Interfaces. *Adv. Colloid Interface Sci.* **1991**, *37*, 1−32.
(37) Temkin, M. I. Adsorption Equilibrium and Kinetics of Process on Non-Homogeneous Surfaces and in the Interaction between Adsorbed Molecules. *Zh. Fiz. Chim.* **1941**, *15*, 296−332.
(38) Reed, D. A.; Ehrlich, G. Surface Diffusion, Atomic Jump Rates and Thermodynamics. *Surf. Sci.* **1981**, *102*, 588−609.
(39) Hill, T. L. *Statistical Mechanics: Principles and Selected Applications*; Dover Publications: New York, 1987.
(40) Fainerman, V. B.; Miller, R. Surface Tension Isotherms for Surfactant Adsorption Layers Including Surface Aggregation. *Langmuir* **1996**, *12*, 6011−6014.
(41) Fainerman, V. B.; Aksenenko, E. V.; Kovalchuk, V. I.; Mucic, N.; Javadi, A.; Liggieri, L.; Ravera, F.; Loglio, G.; Makievski, A. V.; Schneck, E.; et al. New View of the Adsorption of Surfactants at the Water/Alkane Interface — Competitive and Cooperative Effects of Surfactant and Alkane Molecules. *Adv. Colloid Interface Sci.* **2020**, *279*, 102143.
(42) Ori, G.; Villemot, F.; Viau, L.; Vioux, A.; Coasne, B. Ionic Liquid Confined in Silica Nanopores: Molecular Dynamics in the Isobaric−Isothermal Ensemble. *Mol. Phys.* **2014**, *112*, 1350−1361.
(43) Falk, K.; Pellenq, R.; Ulm, F. J.; Coasne, B. Effect of Chain Length and Pore Accessibility on Alkane Adsorption in Kerogen. *Energy Fuels* **2015**, *29*, 7889−7896.